

The Effect of Aerosol Shape in Retrieving Optical Properties of Cloud Particles in the Planetary Atmospheres from the Photopolarimetric Data. Jupiter

Zh. M. Dlugach* and M. I. Mishchenko**

*Main Astronomical Observatory of the National Academy of Sciences of Ukraine, 27 Zalotny ul., Kiev, 03680 Ukraine

**NASA Goddard Institute for Space Studies, 2880 Broadway, New York, NY, 10025 USA

Received February 20, 2004

Abstract—The influence of the assumed shape of aerosols on the estimates of the refractive index and size of particles (based on the data of ground-based spectropolarimetric measurements) is investigated for Jupiter's cloud layer. In the present analysis, we supposed the atmospheric particles to be chaotically oriented spheroids and cylinders with a gamma size distribution. Their single-scattering characteristics were calculated with the T-matrix method, and the intensity and degree of linear polarization of the radiation reflected by the center of the planetary disk were found by solving the vector radiative-transfer equation with consideration for multiple scattering in a plane-parallel atmosphere. We considered a spectral interval from 0.423 to 0.798 μm and phase angles α from 0° to 11° . It has been shown that, if we use the optical characteristics of aerosols found within the frames of a spherical model (Mishchenko, 1990a), the models with the nonspherical particles considered here cannot fit the observational data. The refractive index and the sizes of spheroidal and cylindrical particles were estimated from a comparison of the data of measurements and calculations, and the simplest models for the Jovian cloud layer structure have been considered. We have concluded that the optical parameters of cloud particles (specifically, the refractive index) cannot be reliably estimated only on the basis of measurements made in a narrow range of phase angles.

INTRODUCTION

Polarimetry is one of the most common astrophysical methods for investigating different objects and planetary atmospheres in particular. Polarimetric studies of the Solar System were initiated by Lyot (1929). Between 1960 and 1980, a great number of measurements of the degree of linear polarization of the radiation reflected by the atmospheres of Venus, Mars, Jupiter, and Saturn were carried out (see, e.g., Coffeen and Gehrels, 1969; Dollfus and Coffeen, 1970; Bugaenko *et al.*, 1972; Morozhenko, 1976). A great deal of interest in planetary investigations of this kind was stimulated by the new possibility of really fulfilling a rigorous quantitative analysis of polarimetric observational data. Specifically, the multiple-scattering calculations done for cloudy atmospheres composed of spherical particles showed that the polarization of the light scattered in a planetary atmosphere is extremely sensitive to such properties of aerosols as particle size and refractive index; i.e., these atmospheric parameters can be derived from the interpretation of polarimetric measurements. The pioneering studies in this direction were done by Coffeen (1969) and Hansen and Hovenier (1974) on the atmosphere of Venus. A similar analysis was performed for the atmospheres of Jupiter and Saturn and for the dust cloud on Mars during the dust storm peak in 1971 (Morozhenko and Yanovitskij, 1973; Dollfus *et al.*, 1974; Bugaenko *et al.*, 1975;

Mishchenko, 1990a). It is worth mentioning that this approach to the analysis of polarimetric data requires the shape of particles to be prespecified; all the works listed above considered the model of spherical aerosol particles and used the Mie theory to calculate the single-scattering characteristics. Another approach to the interpretation of the polarimetric data, in particular that concerning Jupiter, was applied by Smith and Tomasko (1984) and Braak *et al.* (2002). The authors abandoned the determination of the refractive index and the sizes of particles, since the aerosols in the Jovian atmosphere are noticeably nonspherical. Instead, they determined the elements of some parameterized single-scattering matrix on the basis of the polarimetric data from the *Pioneer 10*, *Pioneer 11*, and *Galileo* spacecraft and selected the atmospheric-structure model in which the calculations best agreed with the measurements.

Clearly, the shapes of particles must somewhat affect the accuracy of the estimates of the microphysical characteristics of aerosols obtained from the polarimetric and photometric data analysis. However, the degree of this effect and the quantitative differences between the parameters obtained with the models of spherical and nonspherical particles are still poorly known. For the Martian aerosols, some progress was made by Santer *et al.* (1985), who used laboratory measurements to estimate this effect, and by Petrova (1993), who applied approximate formulas. Note that

the rigorous light-scattering calculations revealed a substantial difference in the estimates of the optical thickness of a layer retrieved from satellite measurements with the models of nonspherical particles (even with a slight deviation from the spherical shape) and equivalent spheres (Mishchenko *et al.*, 1995). Considering the influence of the particle shape on the size and refractive index estimated from rigorous calculations for nonspherical aerosols, we can mention only the paper by Dlugach *et al.* (2002), wherein the authors showed that, for the optically thin atmosphere of Mars containing very small particles (the effective radius is about hundredths of micron), the introduction of spheroidal particles with an axial ratio $E = 2.0$ into the model practically doubles their effective radius compared to that for spheres. As far as we know, for particles comparable in size to the wavelength, the effect of the shape on estimates of the refractive index and size retrieved from photopolarimetric data remains to be analyzed with rigorous methods. We consider this problem in the present paper by the example of Jupiter's atmosphere. The majority of the results obtained here were presented by Dlugach and Mishchenko (2003) at the international conference "Photopolarimetry in Remote Sensing" in September–October 2003 in Yalta.

THE OBSERVATIONAL DATA, THE ATMOSPHERIC MODEL, AND THE CALCULATION METHOD

Following Mishchenko (1990a), we used the data on the linear-polarization degree of the center of Jupiter's disk obtained at wavelengths $\lambda = 0.423, 0.452, 0.504, 0.600,$ and $0.798 \mu\text{m}$ in the interval of phase angles α from 0° to 11° (Morozhenko, 1976), as well as data on the reflectance of Jupiter in a spectral range of $0.300\text{--}1.076 \mu\text{m}$ at $\alpha = 2^\circ$ (Woodman *et al.*, 1979).

We considered the following two simple models of the structure of the Jovian atmosphere: (A) a homogeneous semi-infinite gas–aerosol cloud layer consisting of randomly oriented nonspherical particles, and (B) a two-layer medium, wherein a purely gaseous layer with an optical thickness τ_g is above a homogeneous semi-infinite layer containing chaotically oriented nonspherical particles. The appropriateness of such structural models for application to the Jovian atmosphere in the analysis of the observations mentioned above was specifically grounded by Mishchenko (1990a). To interpret the observations mentioned above, two components I and Q of the Stokes vector \mathbf{I} of the reflected radiation must be calculated. The sought intensity I and the linear-polarization degree $P = -Q/I$ are expressed by the elements R_{11} and R_{21} of the reflection matrix \mathbf{R} in the following manner:

$$I(-\mu, \varphi) = \mu_0 R_{11}(\mu, \mu_0, \varphi - \varphi_0), \quad (1)$$

$$Q(-\mu, \varphi) = \mu_0 R_{21}(\mu, \mu_0, \varphi - \varphi_0), \quad (2)$$

where μ_0 and μ are the cosines of the angles of incidence and reflection of the solar radiation, respectively, and φ_0 and φ are the corresponding azimuths. To find R_{11} and R_{21} , the elements F_{11} and F_{21} of the single-scattering matrix \mathbf{F} must be calculated first.

The rigorous calculation of the single-scattering matrix elements for nonspherical particles with their sizes falling in a so-called resonance region (i.e., slightly larger or slightly smaller than the wavelength of incident radiation) is a very complicated problem. At present, one of the most developed and widely used tools for rigorously computing light scattering by such particles is Waterman's T-matrix approach (for details see, e.g., Mishchenko *et al.* (1996)), which is also accompanied by a publicly available computing code (Mishchenko and Travis, 1998). We used precisely this method for our calculations. Following Mishchenko (1990a), we assumed the gamma particle size distribution

$$f(r) = \text{const} \times r^{(1-3v_{\text{eff}})/v_{\text{eff}}} \exp\left(-\frac{r}{r_{\text{eff}} v_{\text{eff}}}\right), \quad (3)$$

where r is the radius of an equal-surface-area sphere.

For model A, the elements R_{11} and R_{21} of the reflection matrix \mathbf{R} were computed by solving Ambartsumian's nonlinear integral equation (with the method suggested by De Rooij (1985)). For model B, the fast invariant imbedding method described by Mishchenko (1990b) was additionally used to take into account the contribution of the overlaying gaseous layer to the reflected radiation.

CALCULATION RESULTS AND THEIR ANALYSIS

Recall that Mishchenko (1990a) modeled the Jovian atmosphere with a homogeneous semi-infinite cloud layer consisting of spherical particles with gamma size distribution (3) for wavelengths $0.423, 0.452, 0.504, 0.600,$ and $0.798 \mu\text{m}$. The best fit to the polarization phase function measured for the disk center was found for the particle model with the real part of the refractive index $N_r = 1.386$, an effective radius $r_{\text{eff}} = 0.385 \mu\text{m}$ with $0.4 < v_{\text{eff}} < 0.5$, and spectral values of the imaginary part of the refractive index N_i obtained with consideration for the data (Woodman *et al.*, 1979) listed in the second column of Table 1. Figure 1 shows the data of measurements (Morozhenko, 1976) (dots) and the phase curves of the linear-polarization degree $P(\alpha)$ of the disk center computed for the atmosphere containing spherical particles with $v_{\text{eff}} = 0.45$ (solid curves).

Randomly oriented oblate and prolate spheroids and cylinders with an axial ratio E of 1.5 and $1.0/1.5 = 0.666\dots$ were used as nonspherical particles in our model. Recall that $E = a/b$ is a ratio of the lengths of horizontal and rotational axes for spheroids and a diameter-to-height ratio for cylinders. We used the same set of $N_r, N_i, r_{\text{eff}},$ and v_{eff} for the particles of the above shapes and calculated the phase curves of the linear-polarization degree $P(\mu, \mu_0)$ of the radiation reflected

Table 1. Spectral values of the imaginary part of the refractive index N_i for spheres and various nonspherical particles

$\lambda, \mu\text{m}$	Spheres	Spheroids $E = 1.3$	Spheroids $E = 1.5$	Spheroids $E = 1/1.3$	Spheroids $E = 1/1.5$	Cylinders $E = 1.3$	Cylinders $E = 1/1.3$
0.423	0.0012	0.0015	0.0016	0.0019	–	0.0013	–
0.452	0.0010	0.0013	0.0013	0.0014	0.0005	0.0011	0.0008
0.504	0.0007	0.0008	0.0009	0.0010	0.0004	0.0007	0.00065
0.600	0.0006	0.0007	0.0008	0.0009	0.0003	0.0006	0.00055
0.798	0.0025	0.0032	0.0035	0.0038	0.0018	0.0027	0.0028

by a semi-infinite atmosphere (for the center of the planetary disk $\mu_0 = \cos \alpha$, $\mu = 1.0$). The results are also displayed in Fig. 1, where it is seen that the model phase curves of polarization of the disk center for the nonspherical particles under consideration strongly deviate from both the observational data and from the models calculated for spherical aerosols. In order to examine the influence of the increasing nonsphericity, we also showed the models calculated for oblate spheroids with $E = 1.3$ (oblique crosses). As one could expect, they are in better agreement with both the observational results and the models for spherical particles. Thus, we may conclude that the assumed shape of aerosol particles is of great importance for retrieving

their optical parameters from the polarimetric data. In other words, the parameters obtained by Morozhenko and Yanovitskij (1973) and by Mishchenko (1990a) are invalid, at least for a cloud layer containing particles of spheroidal and cylindrical shapes.

As for the value of the first Stokes parameter $I(\mu, \mu_0)$, our simulations showed that, in the range of phase angles considered above (0° – 11°), the intensity of the radiation reflected by the center of Jupiter's disk only weakly depends on particle shape. As an example, the ratio of the intensity $I(\cos \alpha, 1.0)$ of the radiation reflected by a semi-infinite layer consisting of oblate spheroids with $E = 1.5$ ($N_r = 1.386$, $r_{\text{eff}} = 0.385 \mu\text{m}$, and $v_{\text{eff}} = 0.45$) to the corresponding quantity calculated for

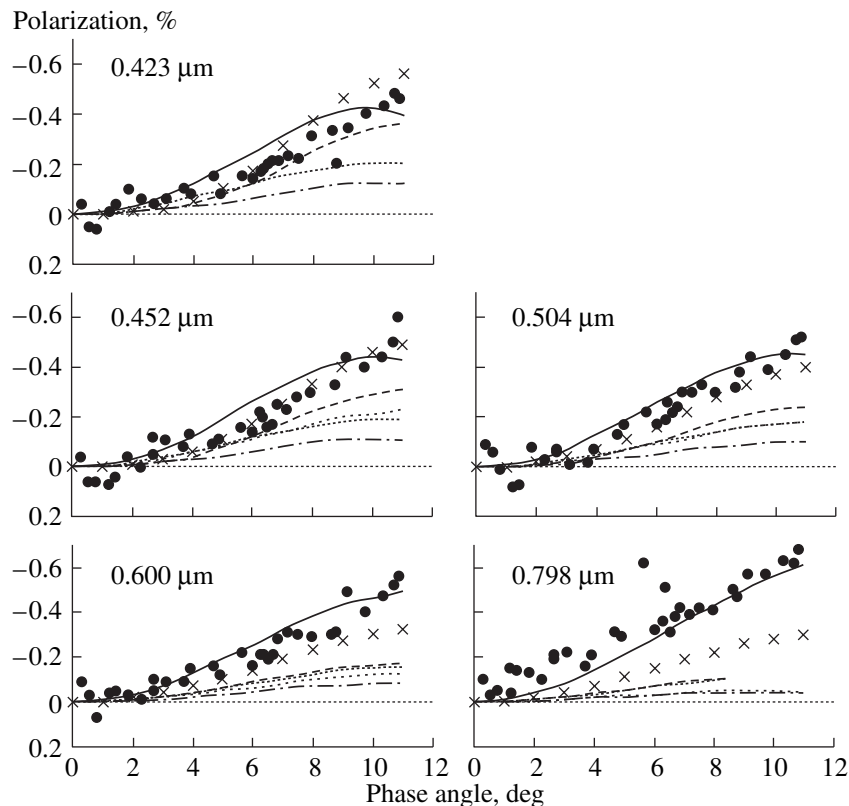


Fig. 1. The phase functions of the degree of linear polarization for the center of Jupiter's disk. (Dots) the results of observations by Morozhenko (1976). (Curves and crosses) the results of model calculations made for the particles of various shapes with $N_r = 1.386$, $r_{\text{eff}} = 0.385 \mu\text{m}$, and $v_{\text{eff}} = 0.45$. (Solid curves) spheres; (long-dash curves) oblate spheroids with $E = 1.5$; (dotted curves) oblate cylinders with $E = 1.5$; (dot-dash curves) prolate spheroids with $E = 1/1.5$; (short-dash curves) prolate cylinders with $E = 1/1.5$; (crosses) oblate spheroids with $E = 1.3$.

Table 2. The ratio $I_{\text{spheroids}, E=1.5}(\cos \alpha, 1.0)/I_{\text{spheres}}(\cos \alpha, 1.0)$

α , degree	0.423 μm	0.452 μm	0.504 μm	0.600 μm	0.798 μm
0	0.99	0.99	0.99	0.99	0.99
1	0.99	0.99	0.99	0.99	0.99
2	0.99	0.99	0.99	0.99	0.99
3	0.99	0.99	0.99	0.99	0.99
4	0.99	0.99	0.99	0.99	0.99
5	0.99	0.99	0.99	0.99	0.99
6	0.99	0.99	0.99	0.99	0.99
7	0.99	0.99	0.99	0.99	0.99
8	0.98	0.98	0.98	0.99	0.99
9	0.98	0.98	0.98	0.99	0.99
10	0.97	0.98	0.98	0.98	0.99
11	0.97	0.97	0.98	0.98	0.98

Table 3. Optical parameters obtained for various nonspherical particles

Shape	E	N_r	r_{eff} , μm	v_{eff}	Model
Spheroids	1.3	1.45	0.35	0.40	B
Spheroids	1.5	1.52	0.40	0.35	B
Spheroids	1/1.3	1.50	0.35	0.30	B
Spheroids	1/1.5	1.54	0.90	0.30	A
Cylinders	1.3	1.43	0.47	0.40	B
Cylinders	1/1.3	1.49	0.60	0.40	B

spherical particles is given in Table 2 for the whole spectral range considered.

Next, we examined a possible influence of particle shape on the estimates of their microphysical characteristics (refractive index and size) derived from photopolarimetric measurements, assuming that the technique applied for spheres was used. We considered particle size distribution (3). For the nonspherical particle shapes, randomly oriented oblate and prolate spheroids with $E = 1.3, 1.0/1.3, 1.5$, and $1.0/1.5$ and cylinders with $E = 1.3$ and $1.0/1.3$ were chosen. The choice of such particles for studying the effect of shape on the scattering properties of aerosols was justified by Mishchenko *et al.* (1995). The measurements by Morozhenko (1976) and Woodman *et al.* (1979) were again used as the observational data. These data were analyzed similarly to Mishchenko (1990a). In this case, at the first stage, the elements of the single-scattering matrix for the ensemble of considered nonspherical particles were computed with the T-matrix method, and thereafter the radiative transfer equation was solved rigorously. As has been mentioned above, two atmospheric models were simulated: (A) a semi-infinite cloud layer consisting of randomly oriented nonspherical particles; (B) a two-layer medium, wherein a purely gaseous layer of an optical thickness τ_g is above a homogeneous semi-infinite layer.

A set of values between 1.3 and 1.8 was tested for N_r . At the first step, we choose the wavelength 0.798 μm and obtained a satisfactory agreement between the modeling results and the observed degree of linear polarization P by varying the parameters N_r , r_{eff} , and v_{eff} . The imaginary part of the refractive index N_i was determined from the comparison of the calculated and measured values of I ; and, as the fulfilled computations showed, it has practically no effect on the calculated value of polarization in the considered range of N_i . Then, for the values of N_r , r_{eff} , and v_{eff} obtained above, we calculated P for $\lambda = 0.600 \mu\text{m}$. In the case of a satisfactory agreement with the measurements, we went on to the next wavelength, $\lambda = 0.504 \mu\text{m}$, and so on. Otherwise, we went back to the wavelength 0.798 μm , found new values of N_r , r_{eff} , and v_{eff} , and calculated again the models for $\lambda = 0.600 \mu\text{m}$ and so on. The process continued until a satisfactory agreement between the measurements and models had been achieved for all the wavelengths tested (0.798, 0.600, 0.504, 0.452, and 0.423 μm). It was found that for all the considered nonspherical particles, except prolate spheroids with $E = 1/1.5$, only model B with an optical thickness of the gaseous layer above the cloud layer equal to $\tau_g(0.423 \mu\text{m}) = 0.2$ (with the corresponding conversion to the other wavelengths according to the spectral behavior of the Rayleigh scattering coefficient) fits the measurements.

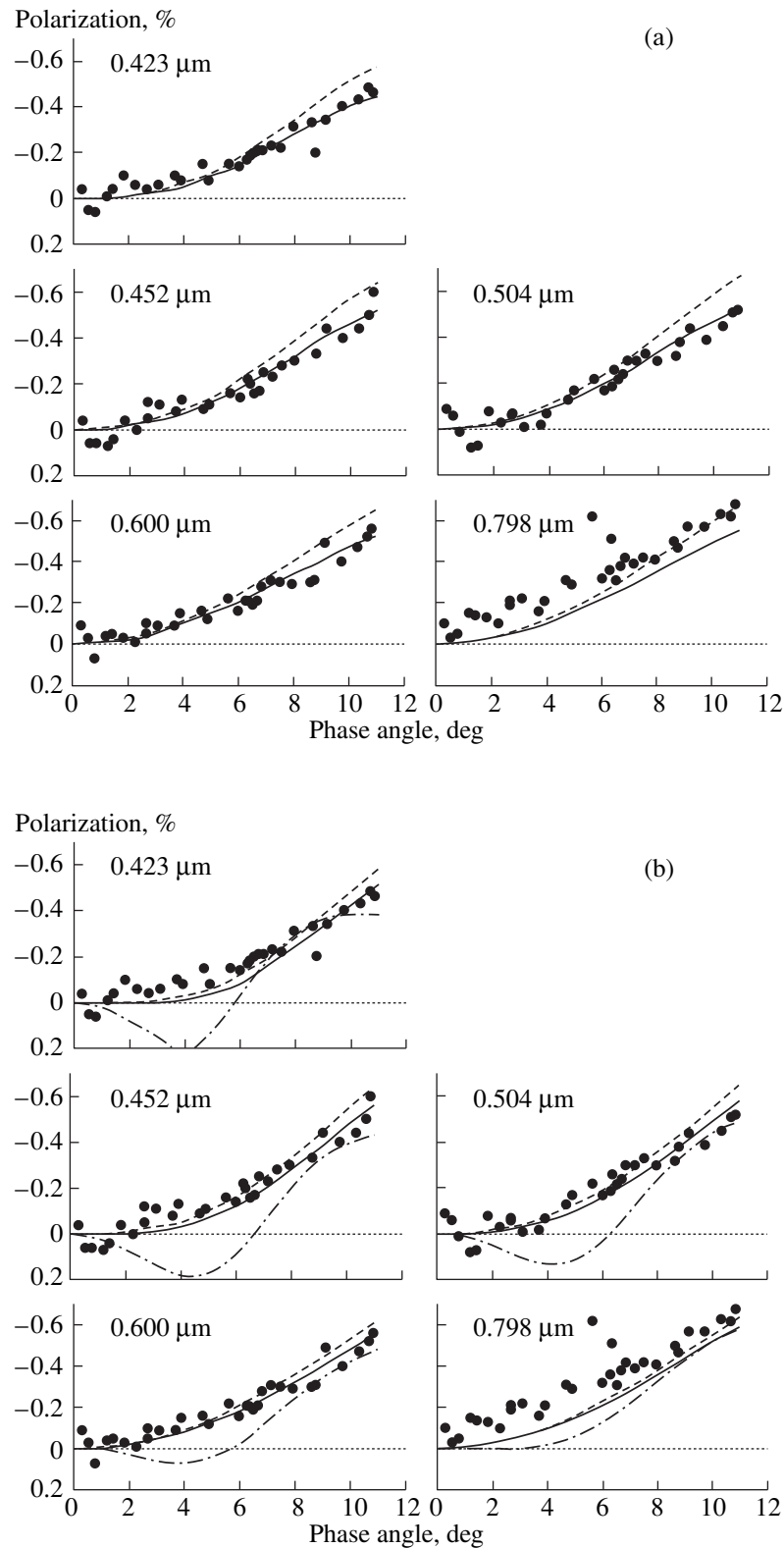


Fig. 2a. As in Fig. 1. The curves present the results of calculations for oblate spheroids with $E = 1.3$. (Solid curves) $N_r = 1.45$, $r_{\text{eff}} = 0.35 \mu\text{m}$, and $v_{\text{eff}} = 0.40$; (dashed curves) $N_r = 1.47$, $r_{\text{eff}} = 0.35 \mu\text{m}$, and $v_{\text{eff}} = 0.40$.

Fig. 2b. As in Fig. 2a. The curves present the results of calculations for oblate spheroids with $E = 1.5$. (Solid curves) $N_r = 1.52$, $r_{\text{eff}} = 0.40 \mu\text{m}$, and $v_{\text{eff}} = 0.35$; (dashed curves) $N_r = 1.54$, $r_{\text{eff}} = 0.40 \mu\text{m}$, and $v_{\text{eff}} = 0.40$; (dot-dash curves) $N_r = 1.42$, $r_{\text{eff}} = 0.80 \mu\text{m}$, and $v_{\text{eff}} = 0.40$.

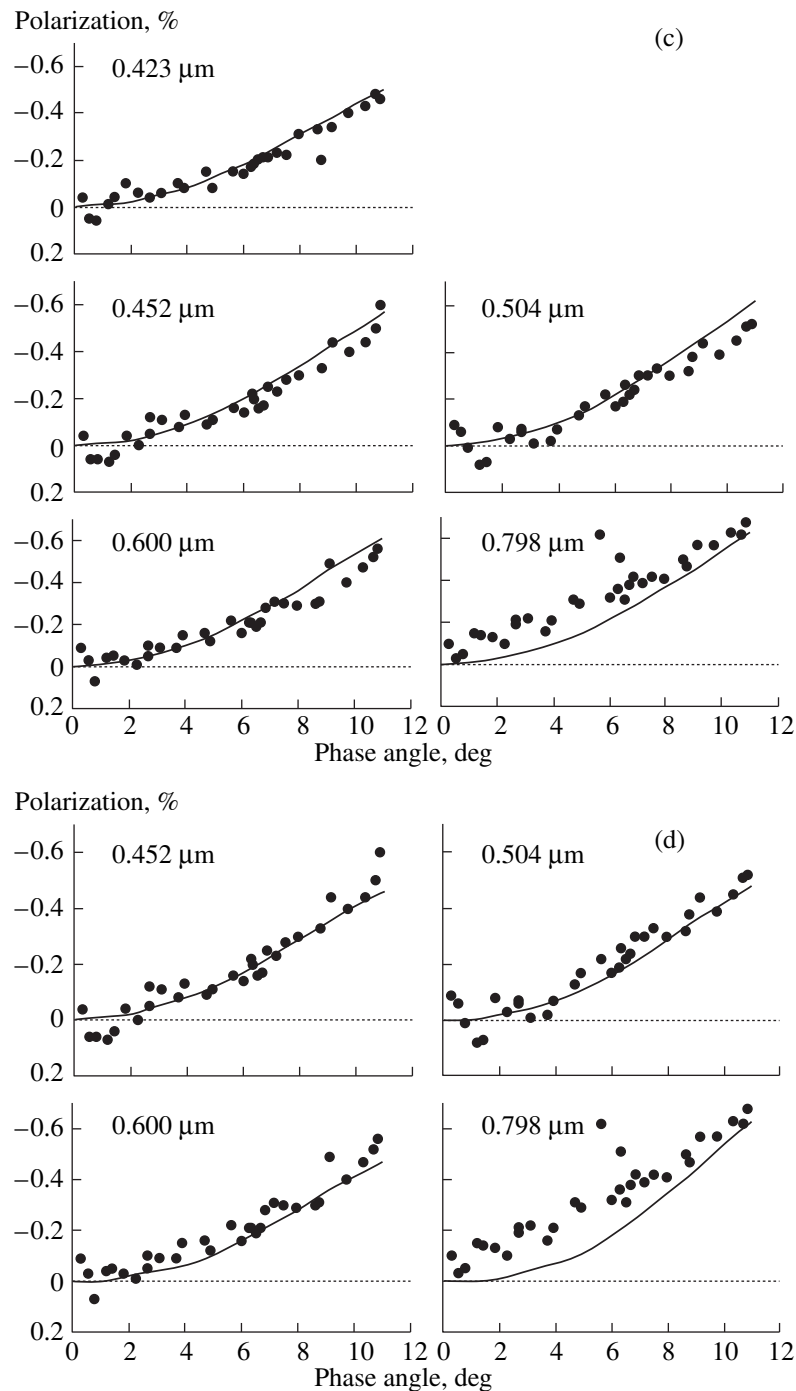


Fig. 2c. As in Fig. 2b. Solid curves present the results of calculations for prolate spheroids with $E = 1/1.3$, $N_r = 1.50$, $r_{\text{eff}} = 0.35 \mu\text{m}$, and $v_{\text{eff}} = 0.30$.

Fig. 2d. As in Fig. 2c. Solid curves present the results of calculations for prolate spheroids with $E = 1/1.5$, $N_r = 1.54$, $r_{\text{eff}} = 0.90 \mu\text{m}$, and $v_{\text{eff}} = 0.30$.

For the case of prolate spheroids with $E = 1/1.5$, model A fits the observations. Note that, unfortunately, the capability of our computers did not allow us to make the T-matrix calculations of the single-scattering matrix elements for prolate spheroids with $E = 1/1.5$ and prolate cylinders with $E = 1/1.3$ at a wavelength of $\lambda = 0.423 \mu\text{m}$.

Table 3 presents the values obtained for the real part of the refractive index N_r , effective radius r_{eff} (the radius of an equal-surface-area sphere), and v_{eff} (the parameter of the particle size distribution); the spectral values of the imaginary part N_i of the refractive index obtained with allowance for the data by Woodman *et al.* (1979) are given in Table 1 (columns 3–8). Figures 2a–2d and

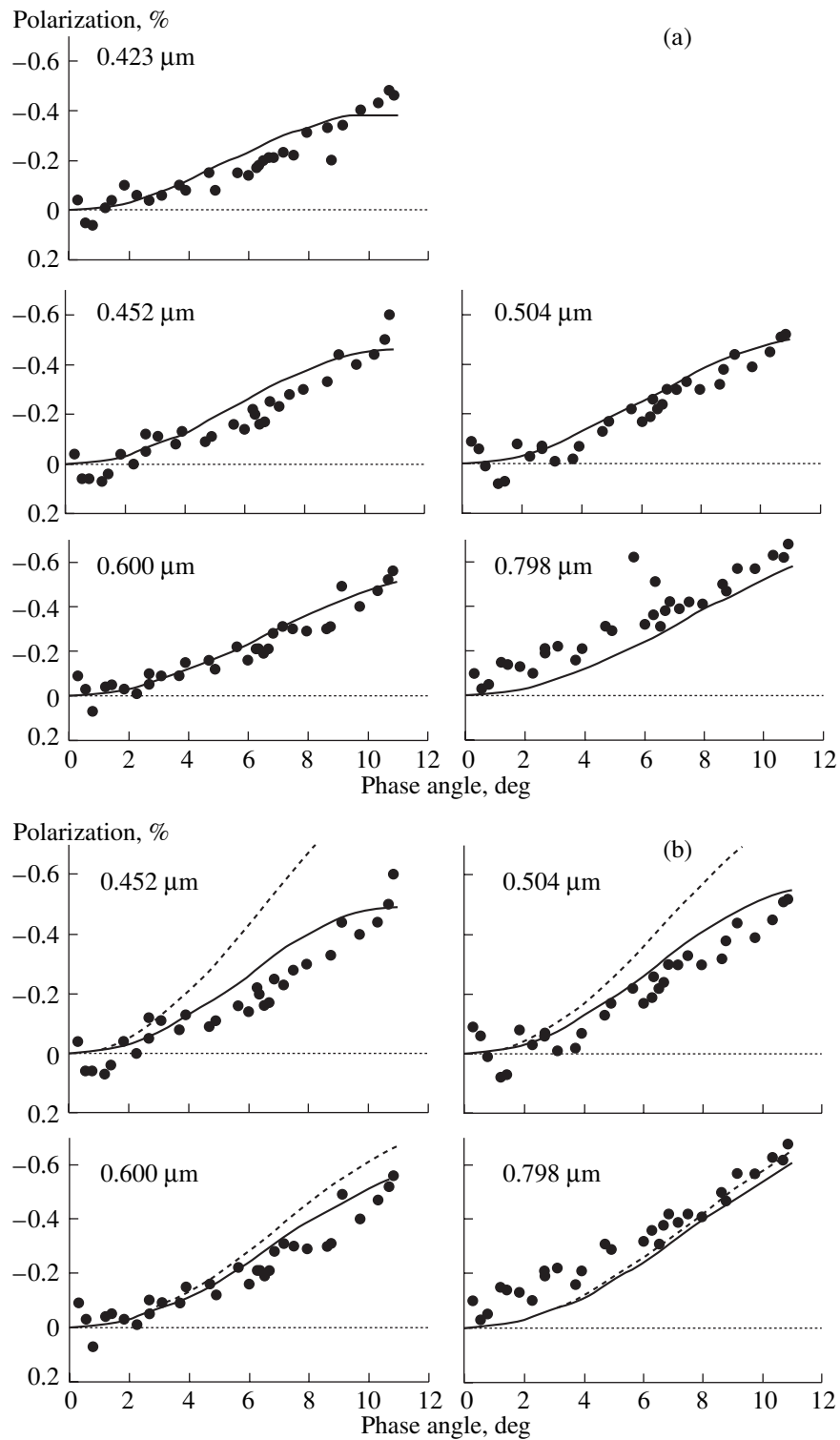


Fig. 3a. As in Fig. 2d. Solid curves present the results of calculations for oblate cylinders with $E = 1.3$, $N_r = 1.43$, $r_{\text{eff}} = 0.47 \mu\text{m}$, and $v_{\text{eff}} = 0.40$.

Fig. 3b. As in Fig. 3a. The curves present the results of calculations for prolate cylinders with $E = 1/1.3$, $N_r = 1.49$, $r_{\text{eff}} = 0.60 \mu\text{m}$, and $v_{\text{eff}} = 0.40$. (Solid curves) atmospheric model B (see text); (dashed curves) $\tau_g = 0$.

3a, 3b show the measured degree of polarization of the center of Jupiter's disk (Morozhenko, 1976) (dots) and the results of our calculations (solid curves) for spheroids (Figs. 2a–2d) and cylinders (Figs. 3a, 3b) with the values of N_r , r_{eff} , v_{eff} , and N_i as given in Tables 3 and 1. It is worth stressing that we did not intend to find the

roids (Figs. 2a–2d) and cylinders (Figs. 3a, 3b) with the values of N_r , r_{eff} , v_{eff} , and N_i as given in Tables 3 and 1. It is worth stressing that we did not intend to find the

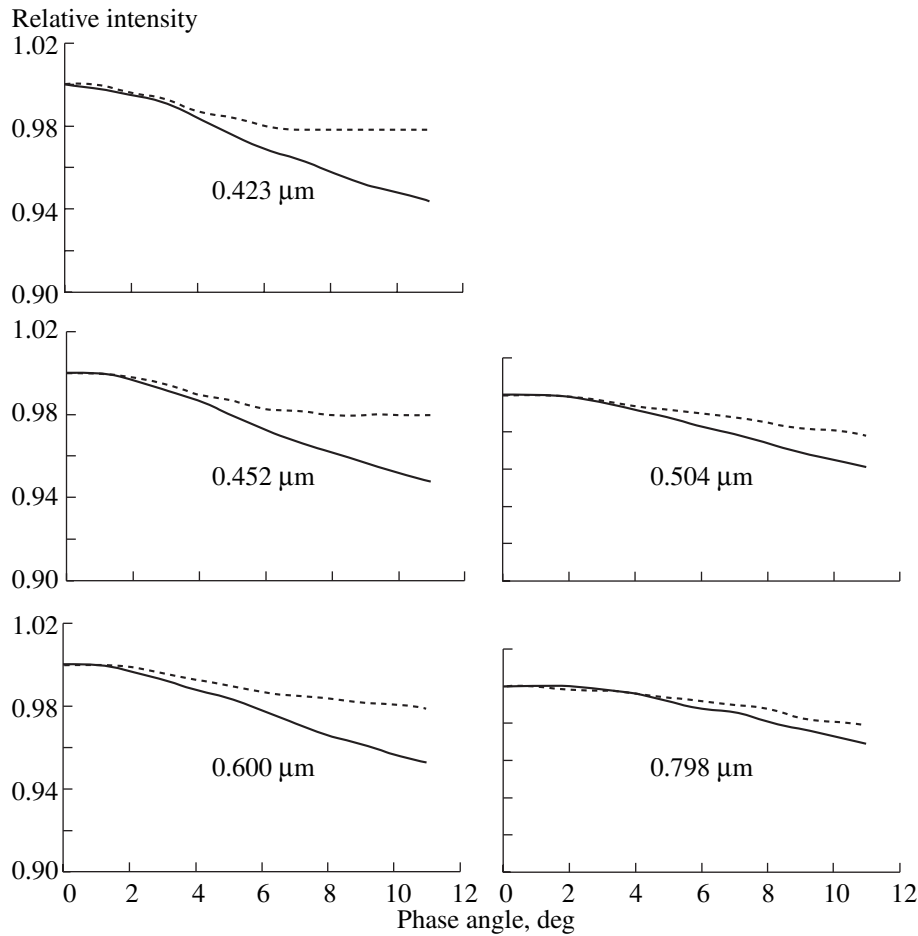


Fig. 4. The model phase curves of relative intensity $I(\cos\alpha, 1.0)/I(1.0, 1.0)$ for the center of Jupiter's disk. (Solid curves) oblate spheroids with $E = 1.5$, $N_r = 1.52$, $r_{\text{eff}} = 0.40 \mu\text{m}$, and $v_{\text{eff}} = 0.35$ (model B); (dashed curves) spheres with $N_r = 1.386$, $r_{\text{eff}} = 0.385 \mu\text{m}$, and $v_{\text{eff}} = 0.45$ (model A).

exact values of the listed parameters (i.e., to also find the errors of their estimates). Our purpose was only to study the problem of the sensitivity of the listed characteristics to the assumed shape of aerosols. However, some ideas on the accuracy of the results obtained can be gathered from Figs. 2a and 2b, where the dashed lines present the models calculated for $N_r = 1.47$, $r_{\text{eff}} = 0.35 \mu\text{m}$, and $v_{\text{eff}} = 0.40$ (Fig. 2a) and $N_r = 1.54$, $r_{\text{eff}} = 0.40 \mu\text{m}$, and $v_{\text{eff}} = 0.30$ (Fig. 2b). In addition, the dot-dash line in Fig. 2b shows the models for $N_r = 1.42$, $r_{\text{eff}} = 0.8 \mu\text{m}$, and $v_{\text{eff}} = 0.40$. It can be seen that there is rather good agreement between the results of measurements and calculations for the phase angles $\alpha = 8^\circ - 11^\circ$; however, for smaller phase angles the model polarization curves begin to deviate strongly from the observational data (the positive polarization branch appears and develops with decreasing wavelength). In order to show the effect of introducing the purely gaseous layer above the cloud layer, the model of a two-layer atmosphere with $\tau_g(0.423 \mu\text{m}) = 0.2$ (solid curves in Fig. 3b) is compared to the model of a one-layer semi-infinite

atmosphere (dashed curves) with the same aerosol parameters.

Thus, the results of modeling (Table 3) showed that even a slight deviation of the particle shape from spherical leads to substantial changes in the optical parameters in comparison to those obtained with the model of spherical aerosols. In the cases considered here, this effect is particularly strong for the real part of the refractive index, and it substantially grows as the nonsphericity increases. For prolate spheroids ($E = 1/1.5$) and cylinders ($E = 1/1.3$), the effective radius also increases noticeably.

As has been mentioned at the beginning of this section, our modeling showed (Table 2) that, for the phase angles ranging from 0° to 12° , the values of the radiation intensity for the center of the planetary disk $I(\cos\alpha, 1.0)$ calculated for spherical and nonspherical particles (specifically, for spheroids with $E = 1.5$) with the same refractive indices and size-distribution parameters practically coincide. It is interesting to estimate the difference between the intensities calculated for the optical parameters of Jupiter's cloud layer found here

and in Mishchenko (1990a). The phase curves of relative intensity $I(\cos\alpha, 1.0)/I(1.0, 1.0)$ calculated for spheroidal particles with $E = 1.5$, $N_r = 1.42$, $r_{\text{eff}} = 0.40 \mu\text{m}$, and $v_{\text{eff}} = 0.35$ in model B of the cloud layer structure (solid lines) and for spherical particles with $N_r = 1.386$, $r_{\text{eff}} = 0.385 \mu\text{m}$, and $v_{\text{eff}} = 0.45$ in model A (dashed curves) are shown in Fig. 4 as an example for comparison. It is seen that there is only a slight difference in the phase curves of intensity for the center of the planetary disk; i.e., the data on the radiation intensity of the disk center obtained at small phase angles are of no use for estimating the shape of cloud particles.

Let us briefly consider the values obtained for the real part of the refractive index N_r . It is common practice to think that the tropospheric layer of Jupiter in large part consists of ammonia ice, the real part of the refractive index of which ranges from 1.417 ($\lambda = 0.940 \mu\text{m}$) to 1.441 ($\lambda = 0.453 \mu\text{m}$) (Martonchik *et al.*, 1984). These values are rather close to N_r as obtained by Mishchenko (1990a). However, this fact hardly evidences the spherical shape of aerosol particles in the Jovian atmosphere. Probably, this coincidence is explained by the fact that the values of the single-scattering parameters F_{11} and $-F_{21}/F_{11}$ for the Jovian aerosols and for the modeled ensemble of spherical submicron particles with this refractive index are close. This can be confirmed by the results of laboratory measurements carried out for ammonia ice crystals (Figs. 4 and 5 in the paper by Pope *et al.*, (1992)). However, it is worth noting that the measurement results for scattering angles $\gamma > 160^\circ$ ($\gamma = \pi - \alpha$), i.e., for the phase-angle range examined here, are absent in the aforementioned paper.

The data presented in Table 3 show that the N_r values obtained here, except the case of $E = 1.3$, substantially differ from those listed above. Probably, this fact shows that the considered particle shapes cannot be used in modeling aerosols in Jupiter's atmosphere. However, we did not state they can, because our purpose was only to investigate how strongly the assumed shape of particles can affect their refractive index and size as estimated from the polarimetric data (in this case, from the phase dependence of polarization of the center of Jupiter's disk). However, it should be stressed that the nature of aerosols in Jupiter's atmosphere is generally unknown. For example, the color of clouds cannot be exclusively explained by the presence of pure ammonia ice. The observed coloring may be caused by some "chromophore" particles present in the atmosphere; they may be mixed with ice particles or covered with ice. This problem was thoroughly discussed in the paper by West *et al.*, (1986), where a multitude of alternatives for this material were considered; however, this subject remains as yet unstudied. However, it seems evident that the presence of admixtures in ammonia clouds must somewhat influence their scattering properties. Consequently, the "overall" refractive index of cloud particles must somewhat differ from that of ammonia ice; i.e., the values of N_r obtained here (Table 3) may be valid to some extent.

CONCLUSIONS

Considering the cloud layer of Jupiter, we found that the assumed shape of atmospheric aerosol particles plays an important part in estimating their optical parameters on the basis of the polarimetric observational results. Our modeling showed that the introduction of spheroidal and cylindrical cloud particles into the model leads to a substantial change (increase) in the real part of their refractive index N_r compared to the value obtained for spherical particles (Mishchenko, 1990a). Moreover, the difference grows as the deviation from a spherical shape increases. In addition, the model of the structure of Jupiter's atmosphere was changed. While for spherical aerosol particles it was possible to fit the measured polarization phase curves with a model of a homogeneous semi-infinite layer, a two-layer atmospheric model (a gaseous layer plus a semi-infinite layer consisting of spheroidal or cylindrical particles) was found to be necessary in most considered cases of nonspherical particles.

Evidently, a lack of information on the particle shape as well as great difficulties (still very often insuperable) connected with the rigorous computing of the single-scattering characteristics for particles of arbitrary shape make, specifically, the possibility of estimating the refractive index (i.e., the nature) of aerosols rather problematic if only the photometric and polarimetric measurements carried out for the center of the planetary disk in a narrow range of phase angles (available for ground-based observations) are used. Probably, spectrophotopolarimetric measurements made in a wide range of phase angles from a spacecraft would yield the additional information required. At the present stage, we can say that it is likely possible only to retrieve the single-scattering characteristics (particularly, the matrix elements F_{11} and F_{21}) for the specified shape of particles and to use them for further modeling and fitting the measurements of the linear polarization degree of the radiation reflected by the planetary atmosphere.

ACKNOWLEDGMENT

The authors are grateful to the referee for careful reading of the manuscript and valuable comments.

REFERENCES

- Braak, C.J., de Haan, J.F., Hovenier, J.W., and Travis, L.D., *Galileo* Photopolarimetry of Jupiter at 678.5 Nm, *Icarus*, 2002, vol. 157, pp. 401–418.
- Bugaenko, O.I., Galkin, L.S., and Morozhenko, A.V., Polarimetric Observations of the Major Planets. II. Phase Dependence of the Polarization for Selected Areas on the Disk of Saturn, *Astron. Zh.*, 1972, vol. 49, pp. 373–379 [*Sov. Astron.*, 1972, vol. 49, p. 837].
- Bugaenko, O.I., Dlugach, Zh.M., Morozhenko, A.V., and Yanovitskii, E.G., Optical properties of Saturn's cloud layer in the visible spectral region, *Astron. Vestn*, 1975, vol. 9, pp. 13–21.

- Coffeen, D.L., Wavelength Dependence of Polarization. XVI. Atmosphere of Venus, *Astron. J.*, 1969, vol. 74, pp. 446–460.
- Coffeen, D.L. and Gehrels, T., Wavelength Dependence of Polarization. XV. Observations of Venus, *Astron. J.*, 1969, vol. 74, pp. 433–445.
- De Rooij, W.A., Reflection and Transmission of Polarized Light by Planetary Atmospheres. *Ph.D. Thesis*, Amsterdam: Vrije Univ., 1985.
- Dlugach, Zh.M., Mishchenko, M.I., and Morozhenko, A.V., The Effect of the Shape of Dust Aerosol Particles in the Martian Atmosphere on the Particle Parameters, *Astron. Vestn.*, 2002, vol. 36, pp. 395–402 [*Sol. Syst. Res. (Engl. Transl.)*, vol. 36, no. 5, pp. 367–373].
- Dlugach, J.M. and Mishchenko, M.I., The Effect of Particle Shape on Physical Properties of the Jovian Aerosols Obtained According Earth-Based Spectropolarimetric Observations, *NATO ASI on Photopolarimetry in Remote Sensing and Workshop on Remote Sensing Techniques and Instrumentation: International cooperation*, Army Research Laboratory, 2003, p. 31.
- Dollfus, A. and Coffeen, D.L., Polarization of Venus. I. Disk Observations, *Astron. Astrophys.*, 1970, vol. 8, pp. 251–266.
- Dollfus, O., Dlugach, Zh.M., Morozhenko, A.V., and Yanovitskii, E.G., Optical properties of the atmosphere and surface of Mars. II. The dust storm, *Astron. Vestn.*, 1974, vol. 8, pp. 211–222.
- Hansen, J.E. and Hovenier, J.W., Interpretation of the Polarization of Venus, *J. Atmos. Sci.*, 1974, vol. 31, pp. 1137–1160.
- Lyot, B., Recherches Sur La Polarisation De La Lumiere Des Planets Et De Quelques Substances Terrestres, *Ann. Obs. Meudon*, 1929, vol. 8, pp. 1–161.
- Martonchik, J.V., Orton, G.S., and Appleby, J.F., Optical Properties of NH₃ Ice from the Far Infrared To the Near Ultraviolet, *Appl. Opt.*, 1984, vol. 23, pp. 541–547.
- Mishchenko, M.I., Physical Properties of the Upper Tropospheric Aerosols in the Equatorial Region of Jupiter, *Icarus*, 1990a, vol. 84, pp. 296–304.
- Mishchenko, M.I., The Fast Invariant Imbedding Method for Polarized Light: Computational Aspects and Numerical Results for Rayleigh Scattering, *J. Quant. Spectrosc. Radiat. Transfer*, 1990b, vol. 43, pp. 163–171.
- Mishchenko, M.I., Lacis, A.A., Carlson, B.E., and Travis, L.D., Nonsphericity of Dust-Like Tropospheric Aerosols: Implications for Aerosol Remote Sensing and Climate Modeling, *Geophys. Res. Lett.*, 1995, vol. 22, pp. 1077–1080.
- Mishchenko, M.I., Travis, L.D., and Mackovski, D.W., T-Matrix Computations of Light Scattering by Nonspherical Particles: A Review, *J. Quant. Spectrosc. Radiat. Transfer*, 1996, vol. 55, pp. 535–575.
- Mishchenko, M.I. and Travis, L.D., Capabilities and Limitations of a Current Fortran Implementation of the T-Matrix Method for Randomly Oriented Rotationally Symmetric Scatterers, *J. Quant. Spectrosc. Radiat. Transfer*, 1998, vol. 60, pp. 309–324.
- Morozhenko, A.V. and Yanovitskii, E.G., The Optical Properties of Venus and the Jovian Planets. I. The Atmosphere of Jupiter According To Polarimetric Observations, *Icarus*, 1973, vol. 18, pp. 583–592.
- Morozhenko, A.V., Results of polarization studies of Jupiter, *Astrometr. Astrofiz.*, 1976, no. 30, pp. 47–54.
- Petrova, E.V., Effect of the nonspherical shape of particles on the estimation of the properties of the aerosol haze on Mars, *Kosm. Issl.*, 1993, vol. 31, pp. 130–135.
- Pope, S.K., Tomasko, M.G., Williams, M.S., *et al.*, Clouds of Ammonia Ice: Laboratory Measurements of the Single Scattering Properties, *Icarus*, 1992, vol. 100, pp. 203–220.
- Santer, R., Deschamps, M., Ksanfomaliti, L.V., and Dollfus, A., Photopolarimetric Analysis of the Martian Atmosphere by the Soviet Mars-5 Orbiter, *Astron. Astrophys.*, 1985, vol. 150, pp. 217–228.
- Smith, P.H. and Tomasko, M.G., Photometry and Polarimetry of Jupiter at Large Phase Angles. II. Polarimetry of the South Tropical Zone, South Equatorial Belt, and the Polar Regions from the *Pioneer 10* and *11* Missions, *Icarus*, 1984, vol. 58, pp. 35–73.
- West, R.A., Strobel, D.F., and Tomasko, M.G., Clouds, Aerosols, and Photochemistry in the Jovian Atmosphere, *Icarus*, 1986, vol. 65, pp. 161–217.
- Woodman, J.H., Cochran, W.D., and Slavsky, D.B., Spatially Resolved Reflectivities of Jupiter During the 1976 Opposition, *Icarus*, 1979, vol. 37, pp. 73–83.